J. Fluid Mech. (1977), *vol.* 80, *part* 1, *pp.* 81–97
Printed in Great Britain

Spatial resonance of a liquid-filled vibrating beaker

By IAN HUNTLEY

Department of Mathematics and Computing, Paisley College of Technology,
Renfrewshire PA1 2BE, Scotland

(Received 12 December 1974 and in revised form 2 September 1976)

Mahony & Smith (1972) put forward a model to explain the phenomenon of energy transfer between nearly resonant oscillations at greatly differing frequencies. However, their model of 'spatial resonance' is restricted to situations where the geometry of the system is very simple. The present paper shows how to derive Mahony & Smith's equations in a general manner, and compares the theoretical predictions for a situation with circular symmetry with existing experimental results (Huntley 1972). In addition, it suggests a simple method for evaluating the resonance frequencies when a liquid-filled beaker is vibrated in one of its bell modes.

1. Introduction

Huntley (1972) presented the results of a series of experiments in which a beaker almost completely filled with water was vibrated continuously near one of its bell-mode resonance frequencies. (These are the gravest elastic vibrations of an open-ended shell: the modes in which a wine glass rings after being tapped.) In certain ranges of the frequency and amplitude of these vibrations large amplitude standing waves were seen to build up in the water, generally reaching an amplitude of several centimetres even though the beaker wall was moving less than a millimetre. The outstanding features of the phenomenon were that the water-wave frequency was always a small fraction (typically about $\frac{1}{50}$) of the excitation frequency, and that if the bell mode had a peripheral wavenumber $k \geqslant 2$ (i.e. there were $2k$ nodes spaced around the circumference of the beaker) then water waves might be generated with a wavenumber of either zero or $2k$. Thus none of the familiar mechanisms for energy transfer between wave modes appeared to be relevant.

In an accompanying paper, Mahony & Smith (1972) put forward a model to explain the transfer of energy through nonlinear coupling between lightly damped, nearly resonant oscillations at greatly differing frequencies, and the phenomenon described by Huntley was thought to be an example of such a 'spatial resonance' phenomenon. For mathematical tractability, however, Mahony & Smith developed their model with respect to a geometrically simple situation (a rectangular enclosure with infinitely deep water), and so a rigorous comparison between the theory and the beaker experiment was not possible. The procedure that was adopted by Huntley, therefore, was to fit the experimental

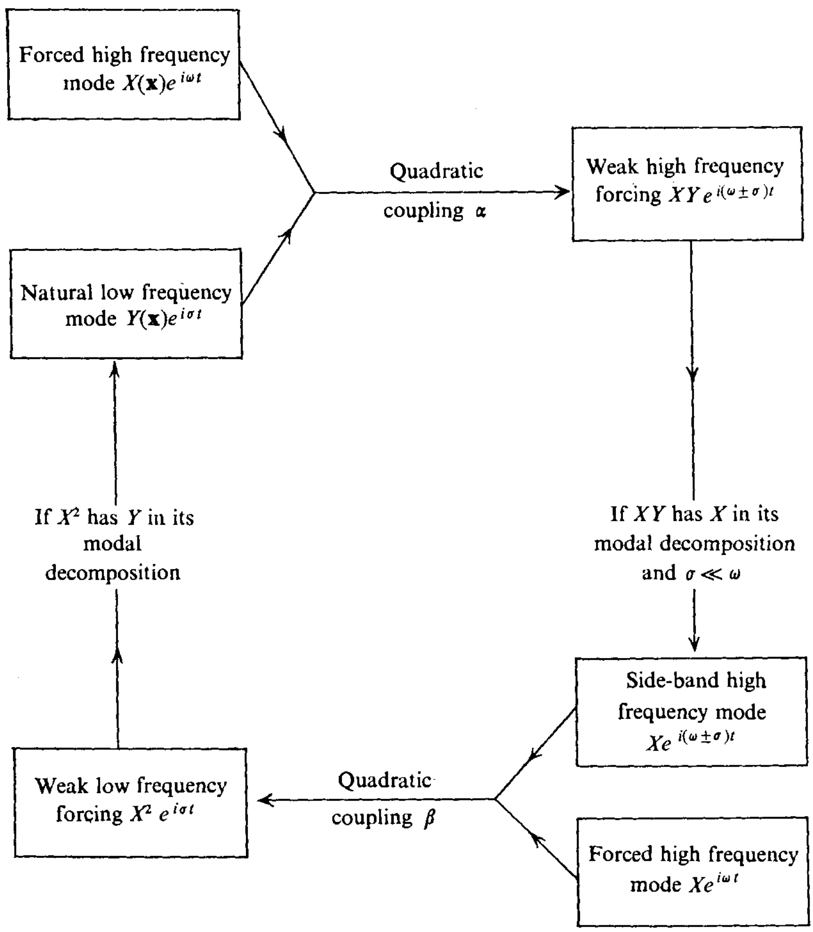

FIGURE 1. Schematic explanation of the Mahony & Smith model.

data to Mahony & Smith's formulae by means of one adjustable parameter. This parameter was the product of the nonlinear coupling coefficients and occurred simply as a proportionality factor in the expression for the neutral-stability curve. (This is the graph against frequency of the critical value of the vibration amplitude above which the high frequency vibrations become unstable and lose energy to the water waves.) Thus although the excellent fit between theory and experiment was strong evidence for the validity of the Mahony & Smith model, nothing was proved.

A schematic explanation of the Mahony & Smith model can be given in terms of the generation of side-band high frequency modes (see figure 1). The system is vibrated at a frequency ω close to the resonance frequency Ω for a particular bell mode with spatial variation $X(\mathbf{x})$. Thus we can expect this mode to dominate the motion. In any real situation, however, we should also expect to have present a small amount of the natural low frequency water wave $Y(\mathbf{x})\,e^{i\sigma t}$. The quadratic coupling between these two modes owing to the nonlinear boundary condition at the (moving) free surface can be interpreted as a weak direct forcing, to which there will be a significant response only when $\sigma \ll \omega$ and thus at least one of the two frequencies $\omega \pm \sigma$ lies within the resonance bandwidth of the high frequency mode. If we assume that the shape of this forcing is not too dissimilar from X, then there will be a significant response in the X mode at one of the side-band frequencies $\omega \pm \sigma$. This side-band mode in turn couples with the driven mode $X\,e^{i\omega t}$ through the Bernoulli pressure condition at the free surface, and provides weak forcing at the frequency σ. This is precisely the frequency of the natural Y mode, and provided that a shape requirement is again satisfied the weak forcing may be able to overcome the natural damping ν' of the wave and so sustain the low frequency mode. It should also be noted that this model automatically leads to a finite threshold for the amplitude of the high frequency drive, below which the natural mode dies away. If we denote the amplitude of $Xe^{i\omega t}$ by $\mathscr{A}$ and that of $Ye^{i\sigma t}$ by $\mathscr{B}$, the diagram shows that the amplitude of the low frequency forcing is proportional to $\mathscr{A}^2\mathscr{B}$. The damping of the low frequency mode, however, is directly proportional to $\mathscr{B}$. Thus for small driving amplitudes the damping dominates, whilst for large amplitudes the nonlinear forcing dominates.

Although the Mahony & Smith model considers only one side-band pair $\omega \pm \sigma$, it is not immediately obvious why other interactions are not included: all the side bands are generated simultaneously, and so a quadratic interaction between the modes $m\omega \pm n\sigma$ and $m\omega \pm (n+1)\,\sigma$ (m, n integral) may be capable of driving the original low frequency water wave at frequency σ. However, for $m \neq 1$ the frequency $m\omega$ is well outside the resonant bandwidth of the high frequency mode Ω and so the response in this mode is effectively zero. Thus we can discount all interactions except those of the form

$$\omega \pm n\sigma,\, \omega \pm (n+1)\,\sigma \rightarrow \sigma \ll \omega,$$

and investigate the relative sizes of these modes. To do this we assume the existence of a water wave whose magnitude is of order δ (thus δ is a small parameter equal to zero initially). If we denote the amplitude of the high frequency mode by $\mathscr{A}(t)$ and that of the low frequency mode by $\mathscr{B}(t)$, then to zero order in δ (i.e. before a wave is present) the solution is just the response to a forcing term F, i.e.

$$d^2\mathscr{A}/dt^2 + \Omega^2\mathscr{A} = Fe^{i\omega t}.$$

This has solution

$$\mathscr{A} = \frac{F}{\Omega^2 - \omega^2}e^{i\omega t} \equiv Ae^{i\omega t},$$

where A is sufficiently small for the linearized theory to hold. Thus

$$\mathscr{A} = Ae^{i\omega t} + O(A^2), \quad \text{say}.$$

This wave will then interact with the infinitesimal water wave $\mathscr{B} = \delta B\,e^{i\sigma t}$, generating the side bands at frequencies $\omega \pm \sigma$. Thus

$$\mathscr{A} = Ae^{i\omega t} + \{A_+\,e^{i(\omega+\sigma)t} + A_-\,e^{i(\omega-\sigma)t}\} + O(\delta^2),$$

where $A_\pm$ are of order δ. To make this ordering more explicit, we may write

$$\mathscr{A} = Ae^{i\omega t} + \delta AB\,e^{i(\omega+\sigma)t}\frac{\lambda_+}{\Omega^2 - (\omega+\sigma)^2} + \delta A\,B^* e^{i(\omega-\sigma)t}\frac{\lambda_-}{\Omega^2 - (\omega-\sigma)^2} + O(\delta^2),$$

where $\lambda_{\pm}$ are interaction coefficients defined via

$$\{\Omega^2-(\omega+\sigma)^2\}A_+ = \lambda_+\,\delta AB,$$
$$\{\Omega^2-(\omega-\sigma)^2\}A_- = \lambda_-\,\delta AB^*,$$

where an asterisk denotes the complex conjugate. The equation governing the low frequency behaviour will now be

$$d^2\mathscr{B}/dt^2+\Sigma^2\mathscr{B} = \{\mu_- A A_-^* + \mu_+ A^* A_+\}\, e^{i\sigma t}+O(\delta^2),$$

where $\mu_{\pm}$ are interaction coefficients and we have shown the terms of order δ explicitly. Thus it is clear that for an onset model ($\delta\to 0$) the only interaction which must be included is

$$\omega,\, \omega\pm\sigma \to \sigma.$$

It is precisely this interaction which is considered in the Mahony & Smith model.

2. Model equations

We consider an idealized situation where the beaker has a rigid base and is full of water, and propose to solve $\nabla^2\Phi = 0$ in the cylindrical region $0\leqslant r\leqslant R$, $0\leqslant\theta\leqslant 2\pi$, $-H\leqslant z\leqslant 0$, where $\Phi(r,\theta,z,t)$ is the velocity potential of the enclosed incompressible inviscid fluid, which is in irrotational motion. It should be noted that since this avoids two major difficulties of the physical system, namely the effect of the glass above the waterline and the effect of the bottom corner on the vibrational modes of the beaker, we are here deriving only approximate model equations for the beaker configuration.

If we denote the undisturbed free surface by $z = 0$ and expand the surface boundary conditions to second order jointly in the velocity potential Φ and the surface displacement ζ about this mean position, we obtain the following results: the surface kinematical condition at $z = 0$ is

$$\Phi_z+\Phi_{zz}\zeta = \zeta_t+\Phi_r\zeta_r+r^{-2}\Phi_\theta\zeta_\theta \qquad (1a)$$

and the dynamical condition at $z = 0$ is

$$\Phi_t+\Phi_{tz}\zeta+\tfrac{1}{2}(\nabla\Phi)^2+g\zeta = 0. \qquad (1b)$$

Similarly, expanding the boundary conditions at the side wall to second order jointly in the velocity potential Φ and the side-wall displacement ξ about the mean position $r = R$, we obtain the kinematical condition on $r = R$ as

$$\Phi_r+\Phi_{rr}\xi = \xi_t+\Phi_z\xi_z+r^{-2}\Phi_\theta\xi_\theta \qquad (1c)$$

and the dynamical condition on $r = R$ as

$$M\xi_{tt}+\kappa\nabla^4\xi = -\Phi_t-\Phi_{tr}\xi-\tfrac{1}{2}(\nabla\Phi)^2+\mathscr{F}, \qquad (1d)$$

where M and κ are physical constants of the boundary shell (M being its mass per unit area and κ its flexural rigidity), the water density has been set equal to unity, and $\mathscr{F}$ represents the external driving force. [It should be noted at this stage that since the linear bending equations can be shown to be reasonable for quite large amplitudes (see Timoshenko & Woinowsky-Krieger 1969, chap. 15), we neglect here any nonlinearities from this source.] To complete the set of boundary conditions, we must add the condition of zero normal velocity at the base of the beaker, i.e.

$$\Phi_z = 0 \quad \text{on} \quad z = -H. \tag{1e}$$

We now intend to use Green's identity

$$\int_{\text{Volume}} \{f\nabla^2 g - g\nabla^2 f\} = \int_{\text{Surfaces}} \left\{ f\frac{\partial g}{\partial n} - g\frac{\partial f}{\partial n} \right\} \tag{2}$$

(where n denotes an outward normal to the surface) to involve the boundary conditions listed above. We set $f \equiv \Phi$ and put g equal to the solution $\hat{\Phi}$ of the linearized system given below. Considering for the moment just the high frequency natural mode and denoting it by $\hat{\Phi}(r, \theta, z)\, e^{i\Omega t}$, we shall have $\nabla^2\hat{\Phi} = 0$ together with the linear boundary conditions:

$$\left.\begin{array}{c} \hat{\Phi}_z = i\Omega\hat{\zeta}, \quad i\Omega\hat{\Phi} + g\hat{\zeta} = 0 \quad \text{on} \quad z = 0, \\ \hat{\Phi}_r = i\Omega\hat{\xi}, \quad -M\Omega^2\hat{\xi} + \kappa\nabla^4\hat{\xi} = -i\Omega\hat{\Phi} \quad \text{on} \quad r = R, \\ \hat{\Phi}_z = 0 \quad \text{on} \quad z = -H, \end{array}\right\} \tag{3}$$

where we have used $\hat{\zeta}$ and $\hat{\xi}$ to denote the surface and side-wall displacements corresponding to the velocity potential $\hat{\Phi}$. [For the low frequency modes we simply replace the resonance frequency Ω by Σ in (3).] Using Green's identity (2) we now have

$$0 = \int_{\text{Top surface}, z=0} \left\{ \Phi_t \frac{\partial\hat{\Phi}}{\partial z} - \hat{\Phi}\frac{\partial\Phi_t}{\partial t} \right\} + \int_{\text{Side walls}, r=R} \left\{ \Phi_t \frac{\partial\hat{\Phi}}{\partial r} - \hat{\Phi}\frac{\partial\Phi_t}{\partial r} \right\}, \tag{4}$$

where we have used the condition of no flow through the base of the beaker. [We note here that the applicability of these equations can be judged by using them in a Galerkin calculation to find the resonance frequencies Ω and Σ. We do this in §4.]

To proceed further we must relate parameters such as Φ and $\hat{\Phi}$, and give an expression for the driving force, which we have denoted above by $\mathscr{F}$. We refer to Mahony & Smith's paper and the discussion in §1 for the appropriate form for Φ, ζ, ξ and $\mathscr{F}$, writing these as

$$\Phi = \{A(t)\, e^{i\omega t} + A_+(t)\, e^{i(\omega+\sigma)t} + A_-(t)\, e^{i(\omega-\sigma)t} + *\}\, \Phi_H \cos m\theta + \{B(t)\, e^{i\sigma t} + *\}\, \Phi_L \begin{Bmatrix} 1 \\ \cos 2m\theta \end{Bmatrix}, \tag{5a}$$

$$\zeta = \{A(t)\, e^{i\omega t} + A_+(t)\, e^{i(\omega+\sigma)t} + A_-(t)\, e^{i(\omega-\sigma)t} + *\}\, \zeta_H \cos m\theta + \{B(t)\, e^{i\sigma t} + *\}\, \zeta_L \begin{Bmatrix} 1 \\ \cos 2m\theta \end{Bmatrix}, \tag{5b}$$

$$\xi = \{A(t)\, e^{i\omega t} + A_+(t)\, e^{i(\omega+\sigma)t} + A_-(t)\, e^{i(\omega-\sigma)t} + *\}\, \xi_H \cos m\theta + \{B(t)\, e^{i\sigma t} + *\}\, \xi_L \begin{Bmatrix} 1 \\ \cos 2m\theta \end{Bmatrix}, \tag{5c}$$

$$\mathscr{F} = \{F e^{i\omega t} + *\} f \cos m\theta. \tag{5d}$$

It should be noted that this expression for $\mathscr{F}$ corresponds to driving the beaker in its $(m-1)$th bell mode at high frequency ω, and that we choose the tangential dependence of the low frequency wave as

$$\begin{Bmatrix} 1 \\ \cos 2m\theta \end{Bmatrix}$$

in order to simulate the wave generated. Here A, $A_{\pm}$ and B are slowly varying functions of time, while Φ_H, Φ_L, ζ_H, ζ_L, ξ_H, ξ_L and f are functions of the radial and vertical co-ordinates r and z, where the subscript indicates a high or low frequency mode.

Using the above representations, we see that to first order (for the high frequency case) we must have

$$\hat{\Phi} = \Phi_H \cos m\theta, \quad \hat{\zeta} = \zeta_H \cos m\theta, \quad \hat{\xi} = \xi_H \cos m\theta. \tag{6}$$

Similarly, when we consider the low frequency case, we must use

$$\hat{\Phi} = \Phi_L \begin{Bmatrix} 1 \\ \cos 2m\theta \end{Bmatrix}, \quad \hat{\zeta} = \zeta_L \begin{Bmatrix} 1 \\ \cos 2m\theta \end{Bmatrix}, \quad \hat{\xi} = \xi_L \begin{Bmatrix} 1 \\ \cos 2m\theta \end{Bmatrix}. \tag{7}$$

Substituting (1) and (3) into the Green's identity (4) then leads us to the governing equation for the high frequency variation:

$$0 = \int_{\text{Top}} [g\Omega^2\hat{\zeta}^2(Ae^{i\omega t}+*) + \Omega^2\hat{\zeta}N_1 + g\hat{\zeta}^2\{(A_{tt}+2i\omega A_t - \omega^2 A)\,e^{i\omega t}+*\} + g\hat{\zeta}\,\partial N_2/\partial t]$$
$$+\int_{\text{Sides}} [\Omega^2\hat{\xi}\kappa\nabla^4\hat{\xi}(Ae^{i\omega t}+*) + \Omega^2\hat{\xi}N_3 + \hat{\xi}\kappa\nabla^4\hat{\xi}\{(A_{tt}+2i\omega A_t-\omega^2 A)\,e^{i\omega t}+*\}$$
$$+(\kappa\nabla^4\hat{\xi} - M\Omega^2\hat{\xi})\,\partial N_4/\partial t],$$

where N_i is used to denote the component of frequency ω of the term

$$\begin{aligned}
&\Phi_{tz}\zeta + \tfrac{1}{2}(\nabla\Phi)^2 && \text{on} \quad z = 0 \quad \text{for} \quad i = 1,\\
&\Phi_r\zeta_r + r^{-2}\Phi_\theta\zeta_\theta - \Phi_{zz}\zeta && \text{on} \quad z = 0 \quad \text{for} \quad i = 2,\\
&\Phi_{tr}\xi + \tfrac{1}{2}(\nabla\Phi)^2 - \mathscr{F} && \text{on} \quad r = R \quad \text{for} \quad i = 3,\\
\text{and} \quad &\Phi_z\xi_z + r^{-2}\Phi_\theta\xi_\theta - \Phi_{rr}\xi && \text{on} \quad r = R \quad \text{for} \quad i = 4.
\end{aligned}$$

We now take account of the slow temporal variation of ζ and ξ, which enables us to ignore second and higher derivatives of linear terms as well as first and higher derivatives of nonlinear terms. The high frequency equation then becomes

$$0 = \int_{\text{Top}} [g\hat{\zeta}^2(\Omega^2-\omega^2)\{Ae^{i\omega t}+*\} + \Omega^2\hat{\zeta}N_1 + g\hat{\zeta}^2\{2i\omega A_t\,e^{i\omega t}+*\} + g\hat{\zeta}\,\partial N_2/\partial t]$$
$$+\int_{\text{Sides}} [\kappa\hat{\xi}\nabla^4\hat{\xi}(\Omega^2-\omega^2)\{Ae^{i\omega t}+*\} + \Omega^2\hat{\xi}N_3 + \kappa\hat{\xi}\nabla^4\hat{\xi}\{2i\omega A_t\,e^{i\omega t}+*\}$$
$$+(\kappa\nabla^4\hat{\xi} - M\Omega^2\hat{\xi})\,\partial N_4/\partial t],$$

where the terms N_i are appropriately simplified forms of the original nonlinear terms. On substituting (6) into the above and performing the θ integrations, we are able to write down very lengthy equations governing the high frequency behaviour when either of the two waves is present in the system.

	1	$\partial_r(\ )$	$\partial_r^2(\ )$	$\partial_z(\ )$	$\partial_z^2(\ )$
			On $r = R$		
Φ_H	$iM\Omega\xi_H$	$i\Omega\xi_H$	$\frac{i\Omega}{R}\xi_H$	$i\Omega\xi_H$	—
Φ_L	$\frac{ig}{\sigma}\zeta_L$	$\frac{ig\sigma}{M\Omega^2}\zeta_L$	$\frac{ig}{\sigma R^2}\zeta_L$	$i\sigma\zeta_L$	—
ξ_L	$\frac{g}{M\Omega^2}\zeta_L$	—	—	$\frac{g\zeta_L}{M\Omega^2 R}$	—
			On $z = 0$		
Φ_H	$\frac{ig}{\Omega}\xi_H$	$\frac{ig}{\Omega R}\xi_H$	—	$i\Omega\xi_H$	$\frac{ig}{\Omega R^2}\xi_H$
Φ_L	$\frac{ig}{\sigma}\zeta_L$	$\frac{ig}{\sigma R}\zeta_L$	—	$\frac{ig}{\sigma R}\zeta_L$	$\frac{ig}{\sigma R^2}\zeta_L$
ζ_H	$1\xi_H$	$\frac{1}{R}\xi_H$	—	—	—

TABLE 1. Magnitudes of the integrands. $\Omega = 836\ \mathrm{s}^{-1}$, $\Sigma = 20{\cdot}9\ \mathrm{s}^{-1}$, $M = 0{\cdot}45\ \mathrm{g\ cm}^{-2}$, $R = 8{\cdot}25$ cm, $\kappa = (6{\cdot}39 \times 10^8)$ dyn cm $\pm 14\%$, $H = 17{\cdot}0$ cm; from Huntley (1973).

Since the equations mentioned above are so lengthy, we should like to be able to pick out the dominant terms. In order to estimate the magnitude of all the terms we must decide on two basic parameters. For these we choose the high frequency wall displacement ξ_H and the low frequency surface displacement ζ_L, since all other terms can be small or have small derivatives in some region. Using the linearized boundary conditions (3), we can now estimate the magnitude of the integrands in the equations in terms of the high and low frequencies Ω and σ. We shall quote the results first, in table 1, and give an explanation of the more complicated estimates afterwards.

These estimates can be obtained by two routes, which in most cases give the same result. One case is more complicated, however, and it is this one that we shall explain in detail. Consider the estimation of $\partial\Phi_L/\partial r$ on the side wall $r = R$. We expect the low frequency part of the velocity potential Φ to be largest near the surface $z = 0$, and so we use the low frequency surface dynamic condition to obtain $\Phi_L \sim (ig/\sigma)\,\zeta_L$. A rough estimate of $\partial\Phi_L/\partial r$ is then $(ig/\sigma R)\,\zeta_L$. To check this we use the low frequency kinematic side-wall condition to obtain the estimate $\partial\Phi_L/\partial r \sim i\sigma\xi_L$ and substitute the value of $\xi_L|_{r=R}$ obtained previously from the dynamic conditions on the side wall. This then gives the quoted result $\partial\Phi_L/\partial r \sim (ig\sigma/M\Omega^2)\,\zeta_L$, which is a significantly better estimate than the previous one. All other terms in table 1 were obtained in a similar, but simpler, manner.

The above estimates then lead us to consider the simplified equations given below, all terms neglected being at least an order of magnitude smaller than those

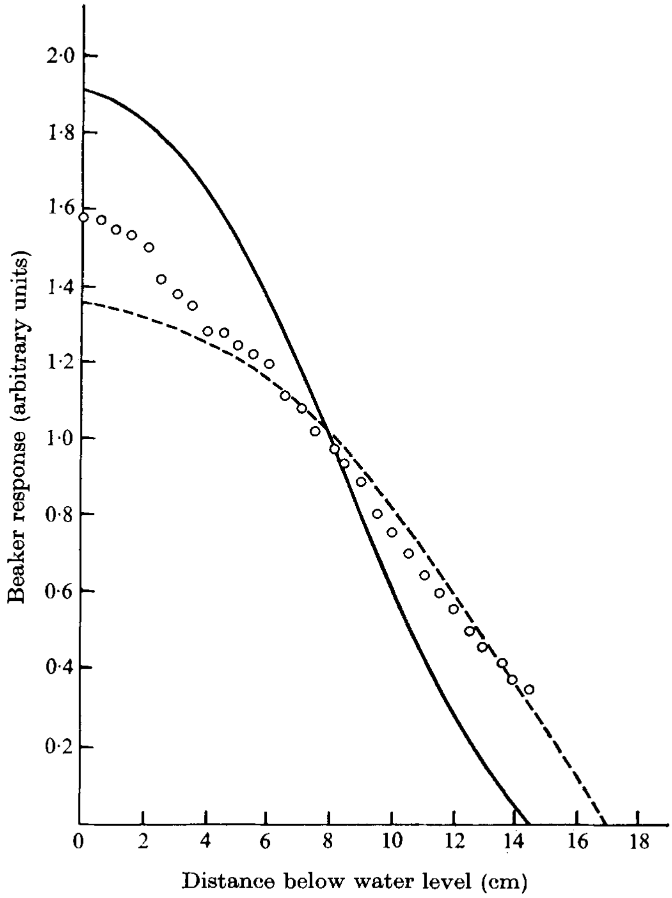

FIGURE 2. Vertical distribution of displacement of beaker side wall. ——, two-term approximation of § 2; – – –, one-term approximation of § 4; ○, experimental point.

retained. For the high frequency behaviour with an axially symmetric wave present, we have

$$0 = i\Omega^3\{A_+B^* + A_-B\}\int_0^R r\zeta_H(\Phi_{Hz}\zeta_L)\,dr + R\kappa\{A(\Omega^2-\omega^2)+2i\omega A_t\}\int_{-H}^0 \xi_H\left(\frac{m^4}{R_4}\xi_H - 2\frac{m^2}{R_2}\xi_{Hzz} + \xi_{Hzzzz}\right)dz - R\Omega^2F\int_{-H}^0 \xi_H f\,dz, \tag{8}$$

and with a cos $2m\theta$ wave present we have

$$0 = \tfrac{1}{2}i\Omega^3\{A_+B^* + A_-B\}\int_0^R r\zeta_H(\Phi_{Hz}\zeta_L)\,dr + R\kappa\{A(\Omega^2-\omega^2)+2i\omega A_t\}\int_{-H}^0 \xi_H\left(\frac{m^4}{R^4}\xi_H - 2\frac{m^2}{R^2}\xi_{Hzz} + \xi_{Hzzzz}\right)dz - R\Omega^2F\int_{-H}^0 \xi_H f\,dz. \tag{9}$$

To evaluate these integrals we must decide how to represent the linear free modes of the system. The displacement of the side walls can be represented by a Fourier cosine series, i.e.

$$\xi_H = \sum_{n=0}^{\infty} \alpha_n \cos\left(\frac{n\pi z}{H}\right),$$

while the velocity potential is composed of terms which correspond to the imposed side-wall displacement together with terms that can be associated with the free-surface displacement. For example,

$$\Phi_H = i\Omega \sum_n \alpha_n \cos\left(\frac{n\pi z}{H}\right) \frac{I_m(n\pi r/H)}{(n\pi/H)\, I_m'(n\pi R/H)} + i\Omega \sum_n \beta_n \frac{\cosh \lambda_n (z+H)}{\lambda_n \sinh(\lambda_n H)} J_m(\lambda_n r),$$

with $J_m'(\lambda_n R) = 0$. In principle we could use truncated forms of these expansions to solve the linear eigenvalue problem (3), and indeed the low frequency surface displacement is well represented by

$$\zeta_L = J_0(\lambda_1 r) \quad \text{or} \quad \zeta_L = J_{2m}(\lambda_1 r), \quad \text{with} \quad \Sigma^2 = \lambda_1 g.$$

For high frequency modes, however, the truncated expansion is not very accurate and so it would seem logical to use the experimentally observed z dependence of ξ_H on $r = R$ to help correct for these simplifications. Setting $\xi_H|_{r=R} = n + \cos(\pi z/H)$ and performing a least-squares fit using the experimental data gives $n = 0{\cdot}91$ and a good fit with the experimental observations (see figure 2).

To evaluate the coefficients β_n we now use a technique very similar to that used earlier. We assume the existence of a function $\Psi(r, \theta, z)$ such that $\nabla^2\Psi = 0$ with $\Psi_r|_{r=R} = 0$ and $\Psi_z|_{z=-H} = 0$. Using Green's theorem, we then have

$$0 = \int_{\text{Volume}} (\Phi\nabla^2\Psi - \Psi\nabla^2\Phi) = \int_{\text{Sides+top+bottom}} (\Phi\Psi_n - \Psi\Phi_n).$$

Thus

$$\int_{\text{Sides}} \Psi\xi = \int_{\text{Top}} \left(\frac{g}{\omega^2}\Psi_z - \Psi\right)\zeta,$$

where we have used the linearized boundary conditions to eliminate $\Phi_r|_{r=R}$, $\Phi|_{z=0}$ and $\Phi_z|_{z=0}$ in favour of ξ and ζ. [This effectively avoids any trouble in the surface integral due to Φ being small on $z = 0$.] We now set

$$\Psi = J_m(\kappa_i r) \cos m\theta\, (\cosh \kappa_i (z+H)/\sinh \kappa_i H),$$

with $J_m'(\kappa_i R) = 0$ for $i = 1, 2, \ldots$. Thus

$$\frac{R J_m(\kappa_i R)}{\sinh \kappa_i H} \int_{-H}^{0} \xi_H \cosh \kappa_i (z+H)\, dz = \frac{1}{i\Omega} \int_0^R r \left(\frac{g\kappa_i}{\omega^2} - 1\right) J_m(\kappa_i r)\, \Phi_{Hz}\, dr.$$

By using the above representations for ξ_H and $\partial\Phi_H/\partial z$, together with the orthogonality of the $J_m(\kappa_i r)$ (see Abramowitz & Stegun 1965, chap. 11), we are able to evaluate the β_n. The first few of these values (for the lowest mode, $m = 2$) are

$$\beta_1 = -4{\cdot}03, \quad \beta_2 = +1{\cdot}94, \quad \beta_3 = -1{\cdot}55.$$

Substituting all these values into (8) and (9) and setting $\Delta \equiv \omega - \Omega$, we obtain the final high frequency model equations. When an axially symmetric wave is present in the system, we have

$$A_t + i\Delta A = \frac{\{A_+ B^* + A_- B\}\,\Omega^4\mathscr{C}_1 + R\Omega^2 F\mathscr{C}_3}{R\kappa i\omega H\left\{\dfrac{m^4}{R^4}(1+2n^2) + 2\dfrac{m^2}{R^2}\dfrac{\pi^2}{H^2} + \dfrac{\pi^4}{H^4}\right\}} \tag{10}$$

whereas when a cos $2m\theta$ wave is present we have

$$A_t + i\Delta A = \frac{\frac{1}{2}\{A_+ B^* + A_- B\}\,\Omega^4\mathscr{C}_2 + R\Omega^2 F\mathscr{C}_3}{R\kappa i\omega H\left\{\dfrac{m^4}{R^4}(1+2n^2) + 2\dfrac{m^2}{R^2}\dfrac{\pi^2}{H^2} + \dfrac{\pi^4}{H^4}\right\}}. \tag{11}$$

Here

$$\mathscr{C}_1 = \int_0^R rJ_0(\lambda_1 r)\{\beta_1 J_m(\kappa_1 r) + \beta_2 J_m(\kappa_2 r) + \dots\}^2\,dr,$$

$$\mathscr{C}_2 = \int_0^R rJ_{2m}(\lambda_1 r)\{\beta_1 J_m(\kappa_1 r) + \beta_2 J_m(\kappa_2 r) + \dots\}^2\,dr$$

and

$$\mathscr{C}_3 = \int_{-H}^0 f\left(n + \cos\frac{\pi z}{H}\right)dz.$$

We must now return to (7) and repeat the previous calculations for the low frequency case. Using the same estimates as previously, we can derive equations analogous to (8) and (9). In this case they coincide (although the representation for ζ_L is different for the two wave modes), and we have

$$0 = 2g\{B(\Sigma^2 - \sigma^2) + 2i\sigma B_t\}\int_0^R r\zeta_L^2\,dr + \Sigma^2\{A_+ A^* + A_-^* A\}\int_0^R r\zeta_L\,\Phi_{Hz}^2\,dr.$$

Using either $\zeta_L = J_0(\lambda_1 r)$ or $\zeta_L = J_{2m}(\lambda_1 r)$ according to the wave present then gives

$$0 = 2g\{B(\Sigma^2 - \sigma^2) + 2i\sigma B_t\}\int_0^R rJ_0^2(\lambda_1 r)\,dr - \Sigma^2\{A_+ A^* + A_-^* A\}\,\Omega^2\int_0^R rJ_0(\lambda_1 r)\{\beta_1 J_m(\kappa_1 r) + \dots\}^2\,dr$$

or

$$0 = 2g\{B(\Sigma^2 - \sigma^2) + 2i\sigma B_t\}\int_0^R rJ_{2m}^2(\lambda_1 r)\,dr - \Sigma^2\{A_+ A^* + A_-^* A\}\,\Omega^2\int_0^R rJ_{2m}(\lambda_1 r)\{\beta_1 J_m(\kappa_1 r) + \dots\}^2\,dr.$$

Setting $\delta \equiv \sigma - \Sigma$ gives us the final low frequency model equations. For an axially symmetric wave we have

$$B_t + i\delta B = \frac{\{A_+ A^* + A_-^* A\}\,\Sigma^2\Omega^2\mathscr{C}_1}{4i\sigma g\mathscr{C}_4} \tag{12}$$

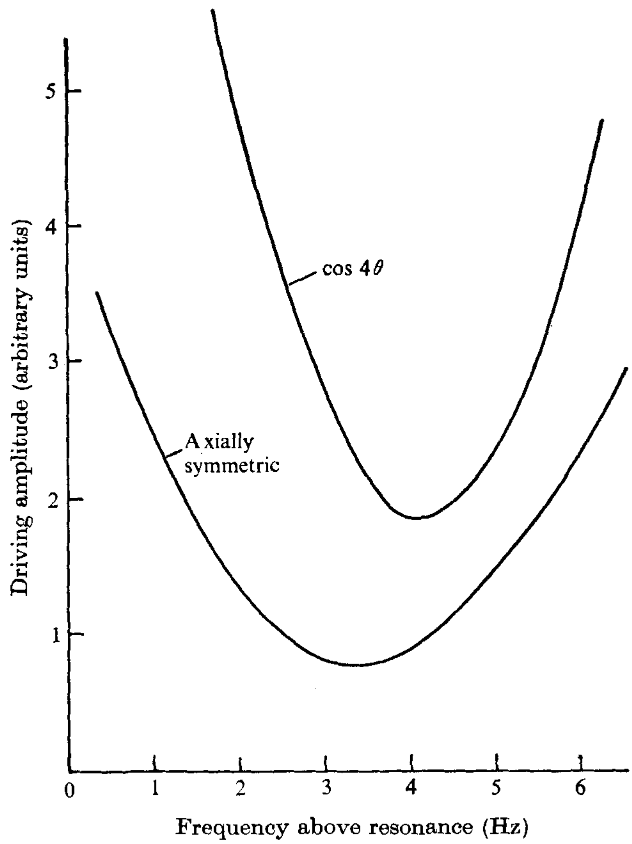

FIGURE 3. Theoretical relation between the neutral-stability curves for the two water-wave modes.

whereas for a cos $2m\theta$ wave we have

$$B_t + i\delta B = \frac{\{A_+ A^* + A^*_- A\}\,\Sigma^2\Omega^2\mathscr{C}_2}{4i\sigma g\mathscr{C}_5}. \tag{13}$$

Here $\mathscr{C}_1$ and $\mathscr{C}_2$ are as defined above, and

$$\mathscr{C}_4 = \int_0^R rJ_0^2(\lambda_1 r)\,dr, \quad \mathscr{C}_5 = \int_0^R rJ_{2m}^2(\lambda_1 r)\,dr.$$

3. Evaluation of the coupling coefficients α and β

By comparing (10)–(13) with the definitions of α and β in Mahony & Smith's paper we can evaluate the coupling coefficients α and β in terms of the $\mathscr{C}_i$. In the present notation, Mahony & Smith's equations become

$$A_t + i\Delta A = \text{drive} + i\alpha(A_+ B^* + A_- B),$$
$$A_{+t} + i(\Delta+\sigma)\,A_+ = i\alpha AB, \quad A_{-t} + i(\Delta-\sigma)\,A_- = i\alpha AB^*,$$
$$B_t + i\delta B = i\beta(A_+ A^* + A^*_- A).$$

[For ease of comparison, we have here omitted the terms due to viscous damping.] So, for the axially symmetric wave, we have

$$\alpha = -\Omega^3\mathscr{C}_1 \Big/ R\kappa H\left\{\frac{m^4}{R^4}(1+2n^2)+2\frac{m^2}{R^2}\frac{\pi^2}{H^2}+\frac{\pi^4}{H^4}\right\}$$

and

$$\beta = -\Sigma\Omega^2\mathscr{C}_1/4g\mathscr{C}_4,$$

whereas for the cos $2m\theta$ wave we have

$$\alpha = -\tfrac{1}{2}\Omega^3\mathscr{C}_2 \Big/ R\kappa H\left\{\frac{m^4}{R^4}(1+2n^2)+2\frac{m^2}{R^2}\frac{\pi^2}{H^2}+\frac{\pi^4}{H^4}\right\}$$

and

$$\beta = -\Sigma\Omega^2\mathscr{C}_2/4g\mathscr{C}_5.$$

[It should be noted that the value of n will depend on the mode m chosen. We are here concerned with $m = 2$, for which $n = 0{\cdot}91$ as explained above.]

Knowing the coupling coefficient $\alpha\beta$, we can now complete the experimental verification using the beaker configuration, and can plot graphically the relationship between the neutral-stability curves for the two different water-wave modes, for comparison with Huntley (1972, figure 5). This is shown in figure 3, where we have used theoretical values of the damping rates given by Case & Parkinson (1957) to construct the neutral-stability curves (Huntley 1972, equations (2)). The theoretical value of $\alpha\beta$ for the axially symmetric wave is $2{\cdot}600\times10^5$ cm^{-4}, whereas the experimental value quoted in Huntley (1973) is $2{\cdot}025\times10^5$ cm^{-4}, so the comparison between theory and experiment is seen to be quite good.

One further comparison between the linear theory and the experiment can be made, by deriving expressions for the high and low resonance frequencies Ω and Σ. This is done in §4.

4. Galerkin calculation for the resonance frequencies of the beaker configuration

We here propose to use the Galerkin method to estimate the high and low resonance frequencies Ω and Σ in the beaker experiments. In order to do this, we must first decide on the appropriate eigenmodes to use. As in the previous section, the r variation of the low frequency surface displacement is well represented by the natural water-wave modes $J_0(\lambda_i r)$ or $J_{2m}(\lambda_i r)$ with $J_0'(\lambda_i R) = J_{2m}'(\lambda_i R) = 0$. Ideally, we should like to represent the high frequency side-wall displacement in terms of the eigenmodes of a clamped–free cylindrical shell, so that $\xi = \xi_z = 0$ at $z = -H$ and $\xi_{zz} = \xi_{zzz} = 0$ at $z = 0$ (see Bickley & Talbot 1961, chap. 14). The analytical description of these modes is not simple, however, and so we seek some form of Fourier representation.

Owing to the nature of a Fourier representation, we can accurately simulate only two of the four edge boundary conditions. For high frequency waves the top and bottom boundary conditions on Φ,

$$\Phi_z = 0 \quad \text{on} \quad z = -H$$

and

$$\Phi_z = (\Omega^2/g)\,\Phi \quad \text{on} \quad z = 0,$$

indirectly impose the conditions

$$\xi_z = 0 \quad \text{on} \quad z = -H$$

and

$$\xi_{zz} \doteqdot 0 \quad \text{on} \quad z = 0.$$

Thus we are free to choose the Fourier representation to satisfy the further conditions

$$\xi = 0 \quad \text{on} \quad z = -H$$

and

$$\xi_{zzz} = 0 \quad \text{on} \quad z = 0.$$

This gives us

$$\xi_H = \sum_0^\infty \alpha_n \cos\left\{(2_n + 1)\frac{\pi z}{2H}\right\}, \tag{14a}$$

which, we note, is not the same representation as that used in §2. However, the comparison between theory and experiment in figure 2 shows it to be an equally valid approximation.

We are now in a position to use the kinematical side-wall condition $\Phi_r|_{r=R} = i\Omega\xi$ and the rigid bottom condition $\xi_z|_{z=-H} = 0$ to find the high frequency series representation for the velocity potential Φ. We have

$$\begin{aligned}\Phi_H = i\Omega \sum_{n=0}^\infty \alpha_n &\left[\frac{\cos\{(2n+1)\pi z/2H\} I_m\{(2n+1)\pi r/2H\}}{(2n+1)(\pi/2H) I_m'\{(2n+1)\pi R/2H\}}\right. \\ &\left.+\sum_{i=1}^\infty \gamma_{ni}\frac{\cosh\lambda_i z}{\lambda_i \sinh\lambda_i H} J_m(\lambda_i r)\right] \\ &+ i\Omega \sum_{i=1}^\infty \beta_i \frac{\cosh\lambda_i(z+H)}{\lambda_i\sinh\lambda_i H} J_m(\lambda_i r),\end{aligned} \tag{14b}$$

where the β_i terms come from the representation of the free-surface displacement as

$$\zeta_H = \sum_i \beta_i J_m(\lambda_i r), \tag{14c}$$

with $\Phi_z = i\Omega\zeta$ on $z = 0$. To evaluate the coefficients γ_{ni} we use the bottom boundary condition $\Phi_z = 0$ on $z = -H$. Then

$$\begin{aligned}0 = \sum_h \alpha_n &\left[\frac{\pi}{2H}(2n+1)(-1)^n \frac{I_m\{(2n+1)\pi r/2H\}}{(2n+1)(\pi/2H) I_m'\{(2n+1)\pi R/2H\}}\right. \\ &\left. - \sum_i \gamma_{ni} J_m(\lambda_i r)\right].\end{aligned}$$

So

$$\begin{aligned}0 = \sum_n \alpha_n &\left[\frac{(-1)^n}{I_m'\{(2n+1)\pi R/2H\}}\int_0^R rJ_m(\lambda_j r) I_m\{(2n+1)\pi r/2H\}\, dr\right. \\ &\left. - \sum_i \gamma_{ni}\int_0^R rJ_m(\lambda_i r) J_m(\lambda_j r)\, dr\right].\end{aligned}$$

These integrals can be evaluated analytically (see Abramowitz & Stegun 1965, chap. 11) to yield the solution

$$\gamma_{nj} = \frac{(-1)^n (2n+1)\pi/H}{R\{1-(m/\lambda_j R)^2\} J_m(\lambda_j R)\{\lambda_j^2 + [(2n+1)\pi/2H]^2\}}. \tag{14d}$$

In a very similar manner, when we are dealing with the axially symmetric low frequency equations we have

$$\xi_L = \sum_0^\infty \alpha_n \cos\left\{(2n+1)\frac{\pi z}{2H}\right\}, \tag{15a}$$

$$\Phi_L = i\Sigma \sum_0^\infty \alpha_n \left[\frac{\cos\{(2n+1)\pi z/2H\} I_0\{(2n+1)\pi r/2H\}}{(2n+1)(\pi/2H) I_0'\{(2n+1)\pi R/2H\}} + \sum_{i=1}^\infty \gamma_{ni}\frac{\cosh\lambda_i z}{\lambda_i \sinh\lambda_i H} J_0(\lambda_i r)\right] + i\Sigma \sum_{i=1}^\infty \beta_i \frac{\cosh\lambda_i(z+H)}{\lambda_i\sinh\lambda_i H} J_0(\lambda_i r), \tag{15b}$$

$$\zeta_L = \sum_i \beta_i J_0(\lambda_i r) \tag{15c}$$

and

$$\gamma_{nj} = \frac{(-1)(2n+1)\pi/H}{R J_0(\lambda_j R)\{\lambda_j^2 + [(2n+1)\pi/2H]^2\}}. \tag{15d}$$

When a $\cos 2m\theta$ wave is present we have

$$\xi_L = \sum_0^\infty \alpha_n \cos\left\{(2n+1)\frac{\pi z}{2H}\right\}, \tag{16a}$$

$$\Phi_L = i\Sigma \sum_0^\infty \alpha_n \left[\frac{\cos\{(2n+1)\pi t/2H\} I_{2m}\{(2n+1)\pi r/2H\}}{(2n+1)(\pi/2H) I_{2m}'\{(2n+1)\pi R/2H\}} + \sum_{=1}^\infty \gamma_{ni}\frac{\cosh\lambda_i z}{\lambda_i \sinh\lambda_i H} J_{2m}(\lambda_i r)\right] + i\Sigma \sum_{i=1}^\infty \beta_i \frac{\cosh\lambda_i(z+H)}{\lambda_i\sinh\lambda_i H} J_{2m}(\lambda_i r), \tag{16b}$$

$$\zeta_L = \sum_i \beta_i J_{2m}(\lambda_i r) \tag{16c}$$

and

$$\gamma_{nj} = \frac{(-1)^n(2n+1)\pi/H}{R\{1-(2m/\lambda_j R)^2\} J_{2m}(\lambda_i R)\{\lambda_j^2 + [(2n+1)\pi/2H]^2\}}. \tag{16d}$$

Calculation for axially symmetric low-frequency wave

For the low frequency modes we are guided by the physical situation to characterize the motion in terms of surface displacements, and so seek to evaluate the α_i series in terms of the β_i. We consider a function Ψ such that $\nabla^2\Psi = 0$ with $\Psi_z = 0$ on $z = -H$, 0; Green's theorem and the bottom boundary condition on Φ then give us the identity

$$0 = \int_{\text{Sides}} (\Phi\Psi_r - \Phi_r\Psi) - \int_{\text{Top}} \Phi_z\Psi,$$

so that

$$0 = 2\pi R\int_{-H}^0 (\Phi\Psi_r - \Phi_r\Psi)\,dz - 2\pi\int_0^R r\Phi_z\Psi dr.$$

Using the linear boundary conditions (3) we can rewrite this as

$$0 = \int_{-H}^0 \left[\left(\frac{K}{\Sigma^2}\nabla^4\xi - M\xi\right)\Psi_r - \xi\Psi\right] dz - \frac{1}{R}\int_0^R r\zeta\Psi\,dr. \tag{17}$$

We now choose

$$\Psi = \frac{I_0\{(2j+1)\pi r/2H\}}{(2j+1)(\pi/2H)I_0\{(2j+1)\pi R/2H\}}\cos\left\{(2j+1)\frac{\pi z}{2H}\right\} + \sum_{i=1}^{\infty}\gamma_{ji}\frac{\cosh\lambda_i t}{\lambda_i\sinh\lambda_i H}J_0(\lambda_i r)$$

and substitute the representations (15) into (17). Finally, we set $j = 0$ and truncate the β_n and γ_{ji} series after one term to obtain

$$0 \doteqdot \alpha_0\left[\frac{\kappa}{\Sigma^2}\left(\frac{\pi}{2H}\right)^4 - M\right]\frac{H}{2} - \alpha_0\frac{I_0\{\pi R/2H\}}{I_0'\{\pi R/2H\}}\frac{H^2}{\pi} - \alpha_0\frac{\gamma_{01}J_0(\lambda_1 R)\pi/2H}{\lambda_1\{\lambda_1^2+(\pi/2H)^2\}} - \beta_1\frac{J_0(\lambda_1 R)}{\{\lambda_1^2+(\pi/2H)^2\}},$$

where we have ignored terms of order $\exp(-\lambda_1 H)$ since the depth H is assumed large. From (15*d*) we can evaluate γ_{01} to get

$$\alpha_0 \doteqdot \frac{\beta_1 J_0(\lambda_1 R)/\{\lambda_1^2+(\pi/2H)^2\}}{\dfrac{H}{2}\left[\dfrac{\kappa}{\Sigma^2}\left(\dfrac{\pi}{2H}\right)^2 - M\right] - \dfrac{H}{2}\left[\dfrac{I_0(\pi R/2H)}{(\pi/2H)I_0'(\pi R/2H)}\right] - \frac{1}{2}\left[\dfrac{(\pi/H)^2}{\lambda_1 R\{\lambda_1^2+(\pi/2H)^2\}^2}\right]}, \tag{18}$$

which we write as $\alpha_0 \doteqdot C_1\beta_1$.

We now consider the free-surface dynamic boundary condition

$$i\Sigma\Phi + g\zeta = 0,$$

and take the $J_0(\lambda_1 r)$ component of this equation to obtain an expression for the resonance frequency Σ. Thus

$$\Sigma^2\left\{\alpha_0\left[\left[\left(\frac{\pi}{2H}\right)I_0'\left(\frac{\pi R}{2H}\right)\right]^{-1}\int_0^R rJ_0(\lambda_1 r)\,I_0\left(\frac{\pi r}{2H}\right)dr + \gamma_{01}\frac{1}{\lambda_1\sinh\lambda_1 H}\int_0^R rJ_0^2(\lambda_1 r)\,dr\right] + \frac{\beta}{\lambda_1}\int_0^R rJ_0^2(\lambda_1 r)\,dr\right\} \doteqdot g\beta_1\int_0^R rJ_0^2(\lambda_1 r)\,dr,$$

which simplifies to

$$\Sigma^2 \doteqdot gRJ_0(\lambda_1 R)\Big/\left\{\frac{RJ_0(\lambda_1 R)}{\lambda_1} + \frac{2C_1}{\lambda_1^2+(\pi/2H)^2}\right\}. \tag{19}$$

We emphasize that this is the (linear) surface wave frequency, taking into account the flexibility of the beaker through the C_1 term. We note that for a rigid beaker we have $\Sigma^2 = g\lambda_1$ as would be expected.

If we now substitute the expression (18) for C_1 and the experimental values quoted earlier into (19), and solve the resulting quadratic in Σ^2, we obtain the theoretical estimate of the resonance frequency as $\Sigma = 3{\cdot}36$ Hz. This compares very well with the experimental value of $3{\cdot}33$ Hz and the value $(g\lambda_1)^{\frac{1}{2}} = 3{\cdot}40$ Hz.

Calculation for $\cos 2m\theta$ *low frequency wave*

We now make a parallel with the work done in the previous subsection and calculate the resonance frequency Σ for the $\cos 2m\theta$ water wave. If we set

$$\Psi = \left\{\frac{I_{2m}\{(2j+1)\pi r/2H\}}{(2j+1)(\pi/2H)I'_{2m}\{(2j+1)\pi R/2H\}}\cos\left\{(2j+1)\frac{\pi z}{2H}\right\} + \sum_i \gamma_{ji}\frac{\cosh\lambda_i z}{\lambda_i\sinh\lambda_i H}J_{2m}(\lambda_i r)\right\}\cos 2m\theta,$$

substitute the representations (16) into (17), and continue as before we obtain

$$\alpha_0 \doteqdot \frac{\beta_1 J_{2m}(\lambda_1 R)/\{\lambda_1^2+(\pi/2H)^2\}}{\frac{H}{2}\left[\frac{\kappa}{\Sigma^2}\left\{\left(\frac{2m}{R}\right)^4+2\left(\frac{2m}{R}\right)^2\left(\frac{\pi}{2H}\right)^2+\left(\frac{\pi}{2H}\right)^4\right\}-M\right]-\frac{H}{2}\left[\frac{I_{2m}}{(\pi/2H)I'_{2m}}\right]-\frac{1}{2}\left[\frac{(\pi/H)^2}{\lambda_1 R\{\lambda_1^2+(\pi/2H)^2\}^2}\right]}$$

$$\equiv C_2\beta_1.$$

Taking the $J_{2m}(\lambda_1 r)$ component of the free-surface dynamic boundary condition then gives the following equation for Σ^2:

$$\Sigma^2 = gRJ_{2m}(\lambda_1 R)\bigg/\left\{\frac{RJ_{2m}(\lambda_1 R)}{\lambda_1}+\frac{2C_2}{\lambda_1^2+(\pi/2H)^2}\right\}.$$

Again, to first order we have $\Sigma^2 = g\lambda_1$ as expected. The theoretical estimate obtained by setting $m = 2$ (as in the experiments) is $\Sigma = 4{\cdot}00$ Hz, which again compares well with the experimental result ($\Sigma = 4{\cdot}10$ Hz) and the value $(g\lambda_1)^{\frac{1}{2}} = 4{\cdot}00$ Hz. We note here that the Galerkin method *for the wave frequencies* is only a little more accurate than the formula $\Sigma^2 = g\lambda_1$.

Calculation for high frequency mode

For the high frequency mode we characterize the motion in terms of side-wall displacements, and seek to evaluate the β_i series in terms of the α_i. To do this we employ the identity

$$0 = R\int_{-H}^{0}\xi\Psi\,dz+\int_0^R r\zeta\Psi\,dr-\frac{g}{\Omega^2}\int_0^R r\zeta\Psi_z\,dr,$$

where
$$\Psi = \left[J_m(\lambda_j r)\frac{\cosh\lambda_j(z+H)}{\cosh\lambda_j H}\right]\cos m\theta,$$

so that $\Psi_z = 0$ on $z = -H$ and $\Psi_r = 0$ on $r = R$. Hence, if we use a one-term representation for ξ it follows that

$$0 \doteqdot \alpha_0\frac{RJ_m(\lambda_j R)}{\cosh\lambda_j H}\int_{-H}^{0}\cos\left(\frac{\pi z}{2H}\right)\cosh\lambda_j(z+H)\,dz + \beta_j\int_0^R rJ_m^2(\lambda_j r)\,dr-\frac{g}{\Omega^2}\lambda_j\beta_j\int_0^R rJ_m^2(\lambda_j r)\,dr,$$

which is an equation for β_j in terms of α_0. If we now ignore small terms such as $g\lambda_j/\Omega^2$ and $1/\cosh \lambda_j H$ we have the approximate expression

$$\beta_j \doteqdot \frac{-2\lambda_j \alpha_0}{RJ_m(\lambda_j R)\left[1-(m/\lambda_j R)^2\right]\left[\lambda_j^2+(\pi/2H)^2\right]}.$$

We now consider the dynamic side-wall boundary condition

$$-\Omega^2 M\xi + \kappa \nabla^4 \xi = -i\Omega\Phi \quad \text{on} \quad r = R.$$

If we substitute into this our expressions for ξ and Φ, and take the cos $(\pi z/2H)$ coefficient of the resulting expression, we obtain an equation for the resonance frequency Ω (where we have again truncated the series representations after one term):

$$\Omega^2\left[M+\frac{I_m(\pi R/2H)}{(\pi/2H)\,I_m'(\pi R/2H)}+\frac{\gamma_{01}\pi J_m(\lambda_1 R)}{2H^2\lambda_1\{\lambda_1^2+(\pi/2H)^2\}}+\beta_1\frac{(2/H)\,J_m(\lambda_1 R)}{\lambda_1^2+(\pi/2H)^2}\right]$$
$$\doteqdot \kappa\left[\left(\frac{m}{R}\right)^4+2\left(\frac{m}{R}\right)^2\left(\frac{\pi}{2H}\right)^2+\left(\frac{\pi}{2H}\right)^4\right]. \quad (20)$$

Substitution of the experimental parameters for the case $m = 2$ into this equation then gives $\Omega = 143{\cdot}08$ Hz, which compares well with the experimental value $\Omega = 133.00$ Hz. It should be noted, however, that the value of κ is fairly inaccurate (Huntley (1973) quotes $\pm 14\%$) owing to irregularities in the thickness of the beaker wall. The total error in the theoretical value is estimated to be about 10%. [An alternative procedure is to use the above equation to evaluate κ. This is done by noting that when the beaker is empty the terms in $I_m(\pi R/2H)$ and $J_m(\lambda_1 R)$ are not present. Thus if we have an experimental value for Ω with the beaker empty, (20) gives an expression for κ. However, great care must be taken to ensure that the truncations used in deriving (20) are still valid.]

The author would like to record his gratitude to Dr R. Smith for help during the course of this investigation and to Dr A. Craik for reading a previous manuscript of this paper.

REFERENCES

ABRAMOWITZ, M. & STEGUN, I. A. 1965 *Handbook of Mathematical Functions*. Dover.

BICKLEY, W. G. & TALBOT, A. 1961 *An Introduction to the Theory of Vibrating Systems*. Oxford University Press.

CASE, K. M. & PARKINSON, W. C. 1957 Damping of surface waves in an incompressible liquid. *J. Fluid Mech.* **2**, 172–184.

HUNTLEY, I. D. 1972 Observations on a spatial-resonance phenomenon. *J. Fluid Mech.* **53**, 209–216.

HUNTLEY, I. D. 1973 Aspects of nonlinear wave interactions. Ph.D. thesis, University of Essex.

MAHOHY, J. J. & SMITH, R. W. 1972 On a model representation for certain spatial-resonance phenomena. *J. Fluid Mech.* **53**, 193–207.

TIMOSHENKO, S. P. & WOINOWSKY-KRIEGER, S. 1969 *Theory of Plates and Shells*. McGraw-Hill.